J Comput Neurosci (2013) 34:303–318
DOI 10.1007/s10827-012-0422-8

Inferring evoked brain connectivity through adaptive perturbation

Kyle Q. Lepage · ShiNung Ching · Mark A. Kramer

Received: 27 April 2012 / Revised: 24 August 2012 / Accepted: 28 August 2012 / Published online: 19 September 2012

Abstract Inference of functional networks—representing the statistical associations between time series recorded from multiple sensors—has found important applications in neuroscience. However, networks exhibiting time-locked activity between physically independent elements can bias functional connectivity estimates employing passive measurements. Here, a perturbative and adaptive method of inferring network connectivity based on measurement and stimulation—so called "evoked network connectivity" is introduced. This procedure, employing a recursive Bayesian update scheme, allows principled network stimulation given a current network estimate inferred from all previous stimulations and recordings. The method decouples stimulus and detector design from network inference and can be suitably applied to a wide range of clinical and basic neuroscience related problems. The proposed method demonstrates improved accuracy compared to network inference based on passive observation of node dynamics and an increased rate of convergence relative to network estimation employing a naïve stimulation strategy.

Keywords Perturbative · Network · Estimation · Functional connectivity · Adaptive

Action Editor: Liam Paninski

K. Q. Lepage and S. Ching contributed to this work equally.

K. Q. Lepage (✉) · M. A. Kramer
Department of Mathematics & Statistics,
Boston University, Boston, MA 02215, USA
e-mail: lepage@math.bu.edu

M. A. Kramer
e-mail: mak@bu.edu

S. Ching
Department of Anesthesia, Critical Care & Pain Medicine,
Massachusetts General Hospital, Boston, MA 02114, USA
e-mail: shinung@neurostat.mit.edu

1 Introduction

A rapidly growing paradigm in neural medicine is the use of brain stimulation for treatment of neurological pathology (Kringelbach et al. 2007). The goal is to directly and non-pharmacologically modulate neuronal dynamics in a manner that ultimately leads to therapeutic effects (Kringelbach et al. 2010; Schiff et al. 2007; Perlmutter and Mink 2006; Moro and Lang 2006). Currently, these technologies are used in a principally open-loop manner, i.e., different stimulation parameters are empirically tested until, eventually, a desired effect is achieved.

A critical component of this neurophysiology is the network connectivity and, specifically, how stimulation at one brain site affects the activity in another. Many inference techniques for neural connectivity are performed in a passive context, measuring and then finding the statistical associations between dynamic activity recorded from separate brain areas. The result is a *functional connectivity* network consisting of nodes (e.g., brain regions or electrodes) and edges typically representing the strongest statistical associations between nodes (reviews in Friston 1994 and Sporns 2010). Such connectivity does not necessarily clarify how stimulation at a network region might affect surrounding regions. Stimulation provides an opportunity to *actively* probe the network and discover these evoked

connections. How to apply this stimulation in a statistically principled and efficient way that yields the maximum information about the underlying network topology—the "evoked network connectivity"—is the question addressed in this paper.

In motivating this work, a specific connection is made to epilepsy, a pathological neurological condition that affects 50 million people worldwide. Of these 50 million, more than 50 % suffer from localization-related epilepsy. Unfortunately, 25–35 % of these patients continue to have seizures despite maximal anticonvulsant therapy (Keränen et al. 1988, 1989; Zarrelli et al. 1999; Annegers 2001), and furthermore those receiving medications may suffer from its considerable side effects. An alternative for patients suffering pharmacologically intractable epilepsy is surgical intervention. This intervention, excision of the brain region generating the seizure (i.e., the seizure focus), relies upon accurate spatial localization. Both noninvasive imaging techniques and invasive voltage recordings made directly from the cortical surface (the electrocorticogram or ECoG) help localize the seizure focus. In many cases, regional surgical resection may reduce or cure seizures but this procedure remains an option of last resort as it carries significant risk and is only curative in $\approx$ 40–70 % of neocortical epilepsy cases (Engel et al. 2003).

The ECoG data—critical for guiding surgical resection and treating epilepsy—also provide a unique window into brain electrical activity. Typical recordings include high density electrode configurations on the cortical surface (e.g., an 8 by 8 electrode grid with 1 cm spacing between electrodes), as well as measurements from deep, mesial brain structures (Gibbs et al. 2002; Schiff et al. 2000, 2005; Alarcon et al. 1995; de Curtis and Gnatkovsky 2009; Fisher et al. 1992).

Recent research has focused on the characterization of functional networks during seizure (see Kramer and Cash 2012, for a review), although the fundamental network characteristics of the seizure remain an active area of research. One difficulty is that the inference of functional networks typically relies on passive observation of brain voltage activity. Such observations cannot distinguish direct causal influences between anatomically connected regions (i.e., "effective connections", Friston et al. 2003) from statistical associations between anatomically unconnected regions (Rubinov and Sporns 2010). For example, statistically inferred associations between the activity recorded at two electrodes can correspond to both a common driving source observed at both electrodes or direct anatomical connections linking the regions observed by the electrodes. In addition, ongoing oscillations, a common phenomenon in neuronal networks, can potentially confound the inferred functional networks (Fig. 1(a)). To obviate these problems, recent work has involved the use of active stimulation applied to ECoG electrodes with implications for understanding brain architecture (Keller et al. 2011), normal brain networks (Matsumoto et al. 2004, 2007; Conner et al. 2011), and brain networks in epilepsy (Enatsu et al. 2012; Valentín et al. 2005a, b). While effective, the stimulus exposes the brain to potentially harmful electric fields. To date, the employed stimulation strategy has not been shown to be optimal.

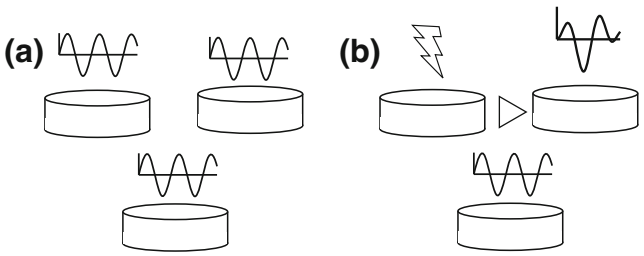

Fig. 1 Schematic of adaptive perturbation scheme for coupled neuronal oscillators. (**a**) In a typical, passive scenario, the functional connectivity between three nodes exhibiting ongoing oscillations is difficult to ascertain. The nodes may be either connected to each other, producing independent activity, or connected to a common driver. (**b**) By using simultaneous stimulation and detection, the connections between nodes can be disambiguated by detecting stimulation effects throughout the network

In this work the inference of brain evoked networks is accomplished with a strategy that performs connectivity estimation as a recursive Bayesian procedure that decouples stimulus/detector design. For each stimulation, an optimal stimulus is chosen according to the current knowledge of the network.

That stimulus is then applied, pairwise tests for connectivity are performed, and subsequent results are used to update network inference for the next stimulation. The strategy, illustrated schematically in Fig. 1(b), is flexible and provides a basis for real-time, optimal network discovery and control.

The paper begins with relevant background in stimulated network estimation in Section 2. The adaptive network inferential procedure is presented in Section 3. Simulations demonstrating the effectiveness of the proposed network estimator are shown in Section 4. The paper ends with a discussion in Section 5.

2 Background

To the best of the authors' knowledge, an adaptive procedure to infer evoked connectivity from brain voltage observations has not been discussed in the litera-

ture. Previous work on stimulated network estimation is related to classical system identification, for example (Juang 1994). This classical work differs from the current work in that the focus in the present work is on inferring connectivity between network nodes as opposed to inferring a dynamical systems model for subsequent use in system control.

The proposed method uses a Bayesian recursive estimator of network connectivity that adaptively changes with time as data and associated stimuli become available. On a superficial level, this procedure is similar to inference conducted with the so-called "time-varying dynamic Bayesian networks" (TV-DBN) (Zhang et al. 2010; Wang et al. 2011).

However, important differences exist. In particular, TV-DBN provides a network model of a joint probability distribution between random variables forming random processes. In this data model, each node is a realization of a random process and a connection between nodes describes a dependence between random processes. The graph describing the network is inferred from data, along with parameters further specifying probabilistic relations, and describes conditional independence between random variables in the model. In the current work, described below, the network edges are the quantities of interest, as opposed to the network nodes, with focus placed upon the edge marginal probability mass functions irrespective of their probabilistic relation to other edges. By directly modeling the quantities of interest (that is the edges, or connections, between nodes), and by further assuming these edges to be probabilistically independent, simplification is obtained and the recursive update avoids considerable computational cost. In particular, a sum over the set of all possible networks connecting a given number of nodes is reduced to two times the number of possible pairwise connections. This is a great reduction in computational burden, from $O(2^{N^2})$ to $O(N^2)$, where N is the number of nodes. In this work, networks are simulated with 24 nodes, and have 276 possible pairwise connections. The number of different networks connecting these 24 nodes is around 10^{83}. In Wang et al. (2011), the number of random processes modeled by a TV-DBN is much less than 24. Determining the feasibility of performing the particle filtering, or sequential Monte-Carlo method of recursive update used in Wang et al. (2011) to infer a TV-DBN on data measured from this modest number of nodes (in terms of ECoG studies) is beyond the scope of the current work. In Zhang et al. (2010), a linear model for node activity is inferred, where the time-dependent coupling matrix captures interactions between nodes. This coupling matrix is estimated via penalized least-squares; highly-connected network estimates are penalized while sparsely connected estimates are preferred. This assumption may not be appropriate for highly-connected networks and is not made herein.

3 Adaptive network inference by perturbation

Adaptive evoked network inference is conducted by updating a prior probability density over all possible networks in a Bayesian inferential framework immediately after the application of a stimulus to a network node. In the current setting, this stimulus is an electric field applied to the brain in the vicinity of an electrode. This stimulus manifests in the voltage waveform and can be subsequently detected in electrode recordings. As demonstrated in simulation in Section 4, this stimulate-record paradigm allows disambiguation of evoked connections from connections inferred amongst, for example, uncoupled synchronous oscillators.

While desirable, adaptive network discovery is problematic given the complexity of the involved data. In a typical paradigm, time-series from n nodes are observed over a recording epoch. Thus, there are $N_{edge} = (n^2 - n)/2$ undirected pairwise connections that may depend on many variables, including time, frequency, and experimental condition. To model the data generation process in a classical statistical fashion that accounts for all manners of connections over the $2^{N_{edge}}$ possible networks is difficult. In this work, the problem is made tractable by decomposing adaptive network discovery into three distinct parts, each part independent of the others when conditioned upon information from previous iterations. These three parts consist of (1) the design and application of the stimulus, (2) the design and application of the "detector", that is, the hypothesis test used to detect the presence of evoked connectivity, and (3) the statistically principled update of the inferred network to reflect the new information acquired during the stimulating and detecting processes. In the proposed paradigm, these three tasks can adapt from one stimulus epoch to another. The following sections detail these three components.

3.1 Stimulus and detector design

In the proposed inferential method, a stimulus at time index k is applied to a node—in this case, an electrode—and a detector is applied pairwise and concurrently to the resulting time-series on all network nodes.

Define a stimulus, **s**, as a vector over all N_{edge} edges, where

$$(\mathbf{s})_j = \begin{cases} 1, & \text{if the jth edge includes a stimulated node} \\ 0, & \text{otherwise} \end{cases}$$

Given s, the detector is assumed to operate with some probability of false alarm, $p_{fa|s}$ and missed detection, $p_{md|s}$. The detector will either detect correspondence between two nodes or will not. Hence the detector response is binary.

Note that, in this paradigm, the stimulus vector s encodes the specific node (electrode) that is stimulated at a given time. It does not describe the specific local stimulus design (e.g. electrical waveform). Such design will be specific to the particular stimulation modality and is not explicitly considered in the proposed methodology. Thus, the notion of "adaptive stimulus" used herein describes *where* a local stimulus, designed *a priori*, should be applied in a broader network.

The detector is assumed to perform identically between any two nodes, depending only on the stimulus type (that is $(\mathbf{s})_j$ equal to 0 or $(\mathbf{s})_j$ equal to 1). The performance of the proposed functional connectivity inferential procedure depends on the performance of the detector. Further, the interpretation of the network depends entirely on what the detector measures. For instance, detectors that are sensitive to high and low frequencies may return different functional networks. Thus, quite abstract notions of evoked networks are possible, depending on the definition of node, stimulus and detector. The general paradigm is depicted in Fig. 1.

In this work, as a specific example of the proposed perturbative network-discovery paradigm, the stimulus is designed to induce sudden and, hence, broad-band, deflections to the node output (waveform). Consequently, the detector is specified to be a frequency-interval energy detector sensitive to unusually large power at high-frequencies, as further described in Section 4 and illustrated by Fig. 2. For this example application of the proposed methodology, a relatively broad-band stimulating pulse directly influences edges such that adjacent nodes possess improbably large energy at high-frequency. Such a situation is distinguishable from uncoupled, or naturally driven oscillations at lower frequencies.

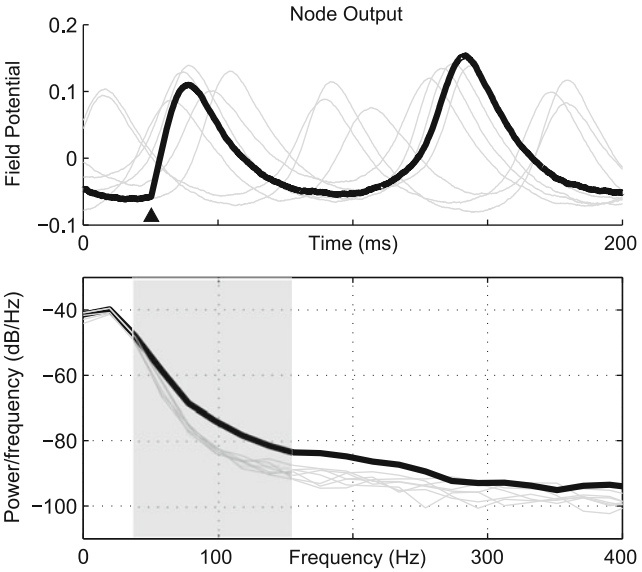

Fig. 2 Example of spectral detector. (*Top*) Waveform output of eight Wilson–Cowan oscillators displaying intrinsic oscillations of similar frequency. A single node (*thick line*) is evoked, causing a sharp broadband deflection (*black arrow*). (*Bottom*) Spectral detection based on high frequency power can be used to detect the broadband increase and, hence, identify the evoked node (*thick line*). The range 40 Hz–150 Hz, shown by the *shaded region*, is used in our simulation

3.2 Adaptive network inference

Define the network, or graph, in terms of two vectors. The first vector, **v**, specifies all possible pair-wise connections. The jth element, $(\mathbf{v})_j$, equals, for example, the pair of integers, (a, b), where a specifies a node (or vertex) in the network, and b specifies another node in the network, potentially connected to node a. Thus, the jth element of the vector **v** defines a potential network connection. The second vector, **e**, contains elements that are either a zero or a one and indicates which of the inter-node connections defined by **v** are present in the network. In particular, if $(\mathbf{e})_j$ equals 1, then the jth pair of vertices specified by the pair of integers, $(\mathbf{v})_j$, are connected. Let **d** be a vector of length N_{edge} containing the result of the connectivity detector described in Section 3.1, applied pairwise to each of the N_{edge} possible network edges, **v**. The detector output for the jth edge, $(\mathbf{d})_j$, is zero if an edge is not detected and it is one if an edge is detected.

Adaptive inference is performed by applying the Chapman–Kolmogorov equation (Papoulis 1984) to the problem of updating the posterior probability distribution of the edges, $P(\mathbf{e}^{(k)}|\mathbf{d}^{(k)}, \mathbf{s}^{(k)}, H_k)$, at stimulus-index k, given the set of observations, $H_k = \{\mathbf{d}^{(a)} \mid a < k\}$, observed during past stimulations. This procedure is similar in spirit to the adaptive filters derived in Eden et al. (2004) for use in the context of non-stimulated, adaptive point-process filtering. Here $\mathbf{s}^{(k)}$ is the vector of N_{edge} elements. Each element is either a zero or a one, indicating if an edge has been stimulated at stimulus-index k, as described in Section 3.1. Note that in the

envisioned paradigm, a stimulus is applied to a specific node and any potential connection emanating from that node is considered stimulated. In Appendix (Section 5.3), it is shown, via the Chapman–Kolmogorov equation, that the edge posterior at stimulus index k can be related to the posterior at stimulus index $k-1$:

$$\begin{aligned}&P\left((\mathbf{e}^{(k)})_j|(\mathbf{d}^{(k)})_j,(\mathbf{s}^{(k)})_j,H_k\right)\\&\propto P\left((\mathbf{d}^{(k)})_j|(\mathbf{e}^{(k)})_j,(\mathbf{s}^{(k)})_j\right)\times\sum_{c_j=0}^{1}P\left((\mathbf{e}^{(k)})_j|(\mathbf{e}^{(k-1)})_j=c_j\right)\\&\times P\left((\mathbf{e}^{(k-1)})_j=c_j|(\mathbf{d}^{(k-1)})_j,(\mathbf{s}^{(k-1)})_j,H_{k-1}\right),\end{aligned}\tag{1}$$

for $j=1,\ \ldots\ ,N_{edge}$. In Eq. (1), the posterior at the previous stimulus index, $k-1$, is updated via multiplication of a user-specified one-step edge update probability mass function, $P\left((\mathbf{e}^{(k)})_j|(\mathbf{e}^{(k-1)})_j\right)$, prior to marginalization and multiplication by the likelihood, $P\left((\mathbf{d}^{(k)})_j|(\mathbf{e}^{(k)})_j,(\mathbf{s}^{(k)})_j\right)$, to yield the posterior probability mass function of the edges at the current stimulus index, k. The one-step edge update probability mass function, $P\left((\mathbf{e}^{(k)})_j|(\mathbf{e}^{(k-1)})_j\right)$, specifies a trade-off between the speed at which the estimates will adapt to a change in the network, and the temporal smoothness of the estimates of the edge as a function of stimulus index. In particular, the one-step edge update is specified as,

$$\begin{aligned}&P\left((\mathbf{e}^{(k)})_j=a|(\mathbf{e}^{(k-1)})_j=b\right)\\&=\begin{cases}a\epsilon+(1-a)(1-\epsilon)\ ,\ b=0\\a(1-\epsilon)+(1-a)\epsilon\ ,\ b=1\end{cases}.\end{aligned}\tag{2}$$

Thus, the small, positive, user-specified parameter, ϵ, controls the extent to which previous estimates of an edge are thought to be accurate during the current stimulus index, k. In this work, emphasis is placed upon stimulus and detector design and the adaptive capability of the proposed edge estimator is not explored. Consistent with this focus upon principled stimulus design, ϵ is set to a value near zero indicating confidence that the network is not rapidly changing.

Completing the description of the posterior edge probability mass function requires specification of the likelihood, given edge independence, $\prod_{j=1}^{N_{edge}}P\left((\mathbf{d}^{(k)})_j|(\mathbf{e}^{(k)})_j,(\mathbf{s}^{(k)})_j\right)$, and an initial, prior probability mass function for the edges, $P\left(\mathbf{e}^{(0)}\right)$. This initial probability mass function, $P\left(\mathbf{e}^{(0)}\right)$, is set to 0.5 for all edges, implying uncertainty regarding the presence or absence of edges in the network. The likelihood of the detector responses conditioned upon knowledge of the network and stimulus at stimulus index, k, is the probability of a sequence of independent Bernoulli trials:

$$\begin{aligned}&\prod_{j=1}^{N_{edge}}P\left((\mathbf{d}^{(k)})_j|(\mathbf{e}^{(k)})_j,(\mathbf{s}^{(k)})_j\right)\\&=\prod_{j=1}^{N_{edge}}\begin{cases}P\left((\mathbf{d}^{(k)})_j|(\mathbf{e}^{(k)})_j=1,(\mathbf{s}^{(k)})_j\right)\ ,\ (\mathbf{e}^{(k)})_j=1\\P\left((\mathbf{d}^{(k)})_j|(\mathbf{e}^{(k)})_j=0,(\mathbf{s}^{(k)})_j\right)\ ,\ (\mathbf{e}^{(k)})_j=0\end{cases}.\end{aligned}\tag{3}$$

That is, at stimulus-index k, the detector responses, $\mathbf{d}^{(k)}$, and which edges were stimulated, $\mathbf{s}^{(k)}$ are known, and Eq. (3), is the probability of the observed detector responses for the kth employed stimulation strategy, as a function of the unknown edges, $\mathbf{e}^{(k)}$. Equation (3) can be more clearly written in terms of the probability of missed detection, $p_{md|s}$, given stimulus s,

$$p_{md|s}=P\Big((\mathbf{d}^{(k)})_j=0\mid(\mathbf{e}^{(k)})_j=1,\ (\mathbf{s}^{(k)})_j=s\Big),\tag{4}$$

and the probability of false alarm, $p_{fa|s}$, given stimulus s,

$$p_{fa|s}=P\Big((\mathbf{d}^{(k)})_j=1\mid(\mathbf{e}^{(k)})_j=0,\ (\mathbf{s}^{(k)})_j=s\Big),\tag{5}$$

where $p_{md|s}$ and $p_{fa|s}$ are assumed to be the same for all j. Specifically, from Eqs. (4) and (5), the likelihood, Eq. (3), can be written as,

$$\begin{aligned}&P\big((\mathbf{d}^{(k)})_j=d\mid(\mathbf{e}^{(k)})_j,\ (\mathbf{s}^{(k)})_j=s\big)\\&=\begin{cases}d(1-p_{md|s})+(1-d)\,p_{md|s}\ ,\ (\mathbf{e}^{(k)})_j=1\\dp_{fa|s}+(1-d)(1-p_{fa|s})\ ,\ (\mathbf{e}^{(k)})_j=0\end{cases}.\end{aligned}\tag{6}$$

Equations (3) and (6) define the likelihood in terms of the probability of false alarm and the probability of missed detection, that is, in terms of the metrics specifying detector performance.

While more complicated policies may be chosen, in this paper the selection of which node to stimulate is determined by selecting the node that possesses maximal "node variance". Node variance is defined as the sum of the variances associated with each of the connection probabilities. That is, if the ℓth edge connecting node i to the other nodes exists with an estimated probability of $\hat{p}_{i,\ell}$, the node variance, η_i, is computed according to,

$$\eta_i=\sum_{\ell=1}^{N_{nodes}-1}\hat{p}_{i,\ell}\left(1-\hat{p}_{i,\ell}\right),\tag{7}$$

where

$$\hat{p}_{i,\ell}=P\left((\mathbf{e}^{(k)})_j|(\mathbf{d}^{(k)})_j,(\mathbf{s}^{(k)})_j,H_k\right).\tag{8}$$

where j indexes the connection between node i and node ℓ. Thus, the node variance summarizes the

uncertainty of the edges that would be involved in a stimulation if the stimulation were applied to node i. The specification of the adaptive policy is completed by specifying the node to stimulate, i*,

$$\mathrm{i}^* = \arg\max_{\mathrm{i}} \eta_{\mathrm{i}} \,. \tag{9}$$

3.3 Qualitative performance

The performance of the proposed inferential paradigm depends on i) the number of nodes, ii) the performance of the detector, and iii) the structure of the network. The fraction of edges evoked by stimulating a single node is inversely proportional to the number of nodes. If almost all edges are evoked on any one node stimulation, then the choice of node to stimulate is irrelevant and any advantage of a more intelligent stimulation strategy will be small. Thus, the proposed technique will be more important for larger networks. When the detector performance is very good, on each detection the presence or absence of an edge will be precisely inferred. In this situation, the ability of the proposed stimulation strategy to re-visit nodes with uncertain connections to other nodes will not be overly helpful. Finally, as the probability of false alarm for many detectors can be set (traditionally to 0.05), the parameter that may change is the probability of missed detection. When the probability of missed detection is high, the detections resulting in the absence of edges are uncertain but detections resulting in connecting edges are less so. Thus, the proposed methodology performs well relative to inference methods employing a naïve stimulation strategy when the network is explored with relatively poor detectors and when the network is large and highly connected, and further possesses some isolated nodes with few connections. This latter situation is explored in simulation in Section 4.

4 Simulation

A simulation study is used to demonstrate the performance of the adaptive perturbation scheme. In particular, scheme is used to infer functional networks in two settings: i) a model network of interconnected mean-field neuronal oscillators, and ii) a more abstract probabilistic network model. In both scenarios, adaptive stimulation is implemented according to Eq. (9). The results indicate favorable performance of the proposed scheme as measured by the accuracy of the inferred network as compared with the true connectivity. Moreover, in the presence of an imperfect detector the scheme significantly outperforms a naive "round-robin" type of stimulation approach.

4.1 Cortical network model

A mean-field model network of interacting neuronal oscillators is used to test the adaptive perturbation scheme in a neurophysiologic setting. Each node in the network is a Wilson Cowan neuronal oscillator that describes the neuronal dynamics within a cortical macrocolumn (Destexhe and Sejnowski 2009; Wilson and Cowan 1972). The model takes the form:

$$\begin{aligned}(\dot{\mathbf{x}})_{\mathrm{j}} = &-(\mathbf{x})_{\mathrm{j}} + \left(\mathrm{k_e} - \mathrm{r_e}(\mathbf{x})_{\mathrm{j}}\right) \mathcal{F}\left(\mathrm{c_1}(\mathbf{x})_{\mathrm{j}} - \mathrm{c_2}(\mathbf{i})_{\mathrm{j}}\right. \\ &\left. + \mathrm{C_e}((\mathbf{x})) + \mathrm{P_j(t)}\right) + \mathrm{b_j^e}(\mathbf{u}(\mathrm{t}))_{\mathrm{j}} + \mathrm{w(t)}\,, \end{aligned} \tag{10}$$

$$\begin{aligned}(\dot{\mathbf{i}})_{\mathrm{j}} = &-(\mathbf{i})_{\mathrm{j}} + \left(\mathrm{k_i} - \mathrm{r_i}(\mathbf{x})_{\mathrm{j}}\right) \mathcal{F}\left(\mathrm{c_3}(\mathbf{x})_{\mathrm{j}} - \mathrm{c_4}(\mathbf{i})_{\mathrm{j}}\right. \\ &\left. + C_{\mathrm{i}}((\mathbf{x})) + Q_{\mathrm{j}}(\mathrm{t})\right) + \mathrm{b_j^i}(\mathbf{u}(\mathrm{t}))_{\mathrm{j}}\,, \end{aligned} \tag{11}$$

where $((\mathbf{x})_{\mathrm{j}}, (\mathbf{i})_{\mathrm{j}})$ are, respectively, the activity in excitatory and inhibitory cell populations of the jth node. The physical meaning of the other parameters, along with typical values, are given in Table 1. The function $\mathcal{F}(\cdot)$ is the sigmoid defined by

$$\mathcal{F}(\mathrm{y}) = \frac{1}{1+\exp\left[-\mathrm{a}\left(\mathrm{y}-\theta\right)\right]} - \frac{1}{1+\exp\left(\mathrm{a}\theta\right)}. \tag{12}$$

Table 1 Parameter values for the Wilson–Cowan model

Symbol	Description	Typical value
c_1, c_3	Average number of excitatory synapses per cell	16, 15
c_2, c_4	Average number of inhibitory synapses per cell	12, 3
P, Q	External input to the excitatory, inhibitory subpopulation	[0,1.25], 0
k_e, k_i	The maximum values of the excitatory, inhibitory response functions	1,1
r_e, r_i	The absolute refractory period of the excitatory, inhibitory subpopulations	1,1
a_e, a_i	The value of the maximum slope of the logistic curve for the excitatory, inhibitory subpopulation	1.3, 2
θ_e, θ_i	The position of maximum slope of the logistic curve for the excitatory, inhibitory subpopulation	4, 3.7

The symbols (first column) are described in the second column and typical values are shown in the third column

The network inter-connectivity arises through the functions $C_e(\cdot)$ and $C_i(\cdot)$, where

$$\mathbf{x}^T = [(\mathbf{x})_1\ (\mathbf{x})_2\ \ldots\ (\mathbf{x})_N]^T, \tag{13}$$

is a vector representing the excitatory activity in each node. The connections between nodes are only excitatory. The specific coupling function considered will be

$$C_{x,i}(\mathbf{x}) = k_s \sum_{k \in \mathcal{N}} c_k \cdot (\mathbf{x})_k, \tag{14}$$

where $\mathcal{N}$ denotes the set of all nodes, k_s is the coupling strength and $c_k = 1$ in the presence of a connection. Such coupling is consistent with synaptic transmission that is the dominant mode of connectivity between brain regions (Hasegawa 2005).

The term $(\mathbf{u}(t))_j$ is the exogenous input, used to locally stimulate a given node in the network. The model parameters are chosen so that each unconnected node displays temporal oscillations. Oscillations in neuronal ensembles are ubiquitous in both normal and pathological neurophysiological regimes (Dayan and Abbott 2005).

As discussed above, ongoing oscillations present a challenge for passive functional connectivity inference schemes. Indeed, connectivity based on metrics such as cross-correlation might erroneously return a fully connected network when each node is, in fact, producing independent oscillations of similar frequency (see Fig. 1(a)). Similarly, erroneous connectivity could arise from independent nodes influenced by a common driver. By using adaptive perturbation, these oscillations can be disrupted and, consequently, connections between nodes can be detected (see Fig. 1(b)).

4.2 Stimulus and detector design

The local stimulus for a given node is defined by the pulsatile input

$$(\mathbf{u}(t))_j = \Gamma, \forall t \in [T_{stim}, T_{stim} + \Delta). \tag{15}$$

Here, Δ is the duration of the pulse and T_{stim} is the time of stimulation. Again, in an actual implementation, the stimulus would be chosen according to the particular experimental conditions and be sensitive to constraints such as charge and current balance (Sunderam et al. 2010; Danzl and Moehlis 2008). Note, again, that the proposed adaptive method determines where in the network (the node index j) $(\mathbf{u}(t))_j$ specified in Eq. (15) will be applied, i.e., the structure of the vector s.

For detection, a spectral discriminator is used. Specifically, following each stimulus, a node is considered to be evoked if

$$\int_{f_1}^{f_2} S_j(x)\, dx > \varphi, \tag{16}$$

where $S_j(\cdot)$ is an estimate of the power spectral density of the jth node, f_1, f_2 determine the frequency range examined and φ is an empirical threshold. In other words, a node is considered evoked if an effect is observed immediately following stimulus application in a specified frequency band. Figure 2 demonstrates this detector design. Here, eight nodes are observed in the presence of ongoing oscillations. A ninth node (not shown) is stimulated using Eq. (15), causing one of the eight "target" nodes to be evoked, leading to a sudden deflection in the output (Fig. 2(a)). This effect is detected as high frequency power in the power spectral estimate (Fig. 2(b)). In this case, the spectral estimate has been computed using a 200 ms window beginning with the onset of the stimulus. The estimation parameters are chosen as

$$f_1 = 40\ \text{Hz}, f_2 = 150\ \text{Hz}, \varphi = 1 \times 10^{-5}, \tag{17}$$

and spectral estimation is performed using a standard Welch's method. In our simulation, this detector is robust to the parameters Eq. (17). Again, in general, the exact detector will be designed according to the experiment and stimulus paradigm under consideration.

4.3 Validation with a biophysical model

Consider a nine node network consisting of Wilson–Cowan oscillators with the following parameterization (Wilson and Cowan 1973):

$$\begin{aligned} &c_1 = 16, c_2 = 12, c_3 = 15, c_4 = 3, a_e = 1.3, a_i = 2 \\ &\theta_e = 4, k_d = 2, \theta_i = 3.7, r_e = r_i = 1, \\ &k_e = k_i = 1, b_j^e = b_j^i = 1, P_j(t) = 1.25, Q_j(t) = 0 \end{aligned} \tag{18}$$

with w(t) a Gaussian random process of variance 0.1. The connectivity in the network is prespecified at the outset of each simulation, and edges are bidirectional.

To implement the adaptive scheme, a 200 ms time interval is chosen between successive stimulations, i.e.,

$$T_{stim} = m \times 200(\text{ms}), \tag{19}$$

is the time of the mth stimulation. The pulse intensity is chosen as $\Gamma = 1$. Spectral estimates of the mth set

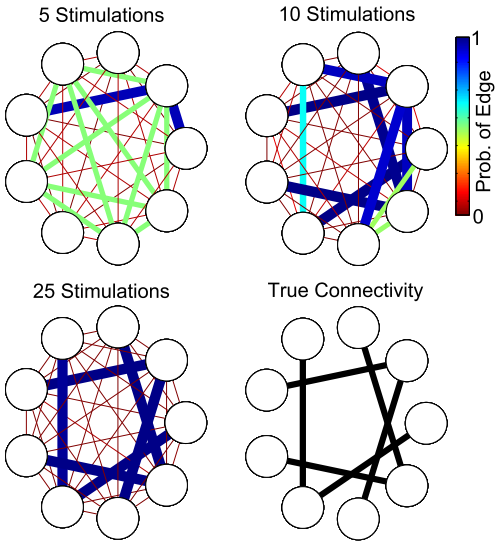

Fig. 3 Inferred connectivity map for a nine node network of neural oscillators. Here, the noise in the model ($\sigma_w^2 = 0.1$) causes the detector to exhibit missed detections with probability around 0.2. The four subpanels show the results of the adaptive scheme after 5, 10, 15 stimulations and the true connectivity. The *colored edges* indicate the probability of appearance determined by the adaptive scheme (*colorbar at right*). Initially, many edges are uncertain (*green*), but the adaptive scheme converges to the correct connectivity in around 25 stimulations

of observations are obtained from the 200 ms interval following stimulation using the parameters in Eq. (17).

Figure 3 shows a particular example of the evolution of the inferred connectivity as a function of the number of stimulations. For the level of noise, w(t), in our model network, the detector offers moderate performance (missed detections occur at a rate of around 0.2, while false alarms occur at a rate of around 0.05). As shown, the correct connectivity is inferred within 25 stimulations.

Figure 4 illustrates the performance in a Monte Carlo simulation for a nine node network with the same detector performance, where the true network connectivity is generated randomly at the start of each trial (each edge is present with equal probability). The correctness of the inferred networks is measured in terms of the Jaccard error, defined as

$$\text{Jaccard Error} = 1 - \frac{|\mathrm{E}_{\text{True}} \cap \mathrm{E}_{\text{Inferred}}|}{|\mathrm{E}_{\text{True}} \cup \mathrm{E}_{\text{Inferred}}|}, \tag{20}$$

where E_{True} and $\mathrm{E}_{\text{Inferred}}$ are the collection of true and inferred edges, respectively. The error takes the value 0 when the inferred network matches exactly the true network. As shown, in the simulation, the inferred connectivity converges to the correct network within 50 stimulations. This figure also illustrates convergence of the mean variance taken over all edges, i.e.,

$$\text{Mean variance} = \frac{1}{\mathrm{N}_{\text{edges}}} \sum_{\mathrm{j}=1}^{\mathrm{N}_{\text{edges}}} \eta_{\mathrm{j}}\,, \tag{21}$$

where η_{j}, the node variance, is defined by Eq. (7). These results demonstrate the efficacy of the scheme in a scenario exhibiting many of the characteristics of observation paradigms such as ECoG or noninvasive scalp electroencephalogram (EEG), with ongoing oscillations and noise contributing to imperfect detector performance. Using our adaptive network discovery scheme, correct networks are inferred with rapid convergence.

4.4 Validation with a probabilistic model

In the biophysical model of the previous section, the applied stimulus altered the dynamics of node activity, as revealed by changes in spectral power. In this section, a detector response, at every stimulus index, is the result of a Bernoulli draw consistent with the probability of detection. That is, the connections between N_{node} nodes in a network are specified to be either present or absent at the beginning of a simulation. At every stimulus

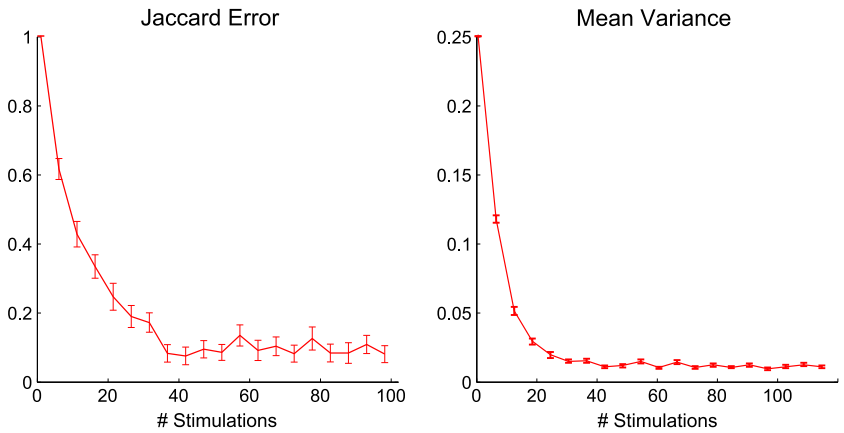

Fig. 4 Monte Carlo simulation ($n = 100$) of nine node network. For each simulation, the network edges are generated randomly and equiprobably. The detector exhibits probability of missed detections around 0.2. The Jaccard distance and mean network variance converge in around 50 stimulations

index, $N_{node} - 1$ Bernoulli draws are made representing the detector response between a stimulated node and the $N_{node} - 1$ nodes to which it may be connected. Each of these draws has a probability of being a 0 or a 1, specified by the likelihood presented in Eqs. (3) and (6). In this way, the proposed methodology is tested and evaluated independently of biophysical effects. These simulations directly compare the proposed methodology with "brute-force" stimulation paradigms.

Simulation 1 involving two parts: For both parts of this simulation, 30 realizations of 24 node, nearly fully-connected networks are realized with all but 69 of the total of 276 possible connections missing. These 69 missing edges are distributed in such a way that, in each realization, a few nodes of the network are predominantly isolated from the rest of the nodes in the network, a network topology that favors the proposed methodology. For each of these realizations, networks are estimated with both the proposed methodology and with a round-robin stimulation strategy employing the same detector and stimulus, but applying the stimulus one node at a time in a round-robin fashion.

For the first part of Simulation 1, the detector probability of missed detection is set to 0.4. In the second part of Simulation 1 this probability is set to 0.1. For each of the 30 realizations, and at each of the 200 stimulation indices, network estimates are computed in two different ways. The first network estimate is computed with the proposed inferential method described in Section 3. The second network estimate is computed by comparing the average of the detector responses up to and including the current stimulation index, on an edge-by-edge basis to a threshold of 0.5. If this average, equal to the maximum likelihood estimate of the probability of an edge (without knowledge of detector performance), is greater than 0.5, an edge is inferred. This latter method of edge inference is paired with the round-robin stimulation strategy and provides a realistic inferential procedure with which the performance of the proposed inferential strategy is compared. The resulting network estimates are compared against the actual network using the Jaccard distance (left, Fig. 5) and by comparing network uncertainty (right, Fig. 5). Here, a network estimate uncertainty comparison is conducted by computing the ratio of the average of the node variance over all nodes for the two proposed network estimates. In this latter comparison, the effect of stimulation strategy is isolated from edge probability estimation by estimating the edge probabilities

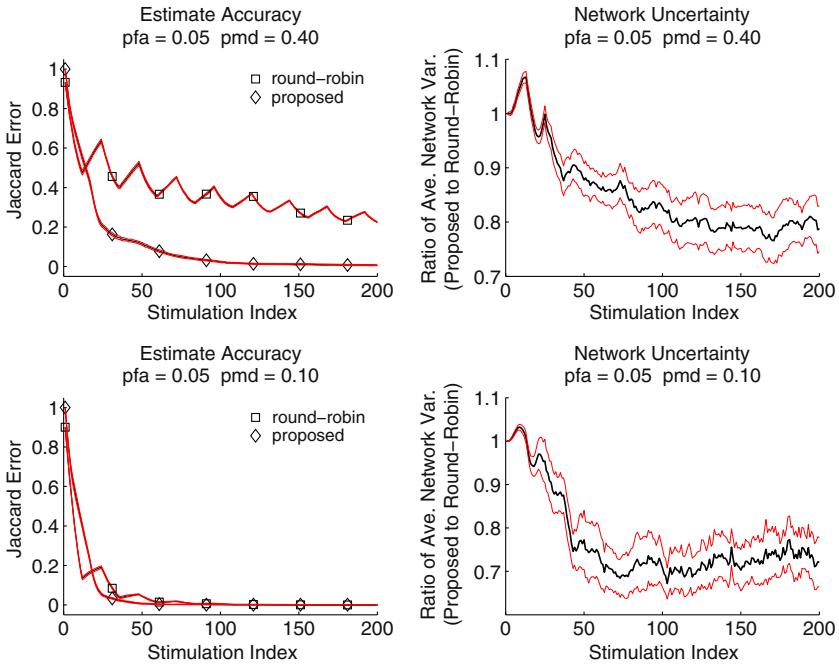

Fig. 5 Accuracy of proposed vs more naïve network inference. For each of 30 realizations, a 24 node network is simulated possessing a total of 276 possible edges. Of these possible edges all are present forming connections between nodes save for 69 which are clustered. Most nodes are fully connected while a few nodes are mostly isolated. The proposed method achieves an accuracy in 20 stimulations that the competing method employing the round-robin stimulation strategy does not attain for another 140 stimulations. *Right*: Network uncertainty comparison. Network variance, equal to the sum of the node variances, is lower when using the proposed method. See text for a definition of node variance

with the proposed recursive scheme for both network estimates but employing the two different stimulation strategies. In the first case (complete, proposed network estimate), the node to stimulate is chosen with the proposed methodology. In the second case, the node to stimulate is chosen according to a round-robin sequential stimulation strategy. Network variance is computed as the sum of the node variances. In all figures in this section the red-band indicates the 95 % confidence interval.

The proposed network estimate does as well or substantially better than the alternative round-robin approach when detector probability of missed detection is 0.4. In particular, the Jaccard error of the network estimate involving the round-robin strategy is over twice that of the proposed method. Network estimates computed with the proposed methodology are more certain than estimates computed with the more naïve approach, regardless of the probability of missed detection (right-half of Fig. 5). As the number of stimulations increases estimate certainty of the proposed network estimator tends to approximately 70–80 % of the network variance of the estimates computed with the more naïve approach. To further investigate the effect of the stimulation strategies, the node variance as a function of stimulation index is presented in Fig. 6.

Simulation 2: The first simulation is repeated but with a network where only a small number of edges are randomly distributed amongst the nodes. This situation is one where the proposed methodology conveys the least advantage since it is difficult to find nodes that will preferentially stimulate the problematic parts of the network, i.e., those parts that are associated with missing connections. Recall that missing connections are more difficult to confidently infer due to the probability of missed detection exceeding the probability of false alarm. The parameters in this simulation are identical to the parameters in Simulation 1, except that the networks possess only 14 edges. Again, this is a situation where the proposed methodology is least effective due to the distribution of uncertain connections across many of the nodes and in large numbers. In this situation a round-robin stimulation strategy will tend to stimulate as many of these uncertain edges as the proposed stimulation strategy. The resulting performance is shown in Fig. 7 (left) and the associated stimulation strategy is shown in Fig. 7 (right). The proposed methodology out-performs the more

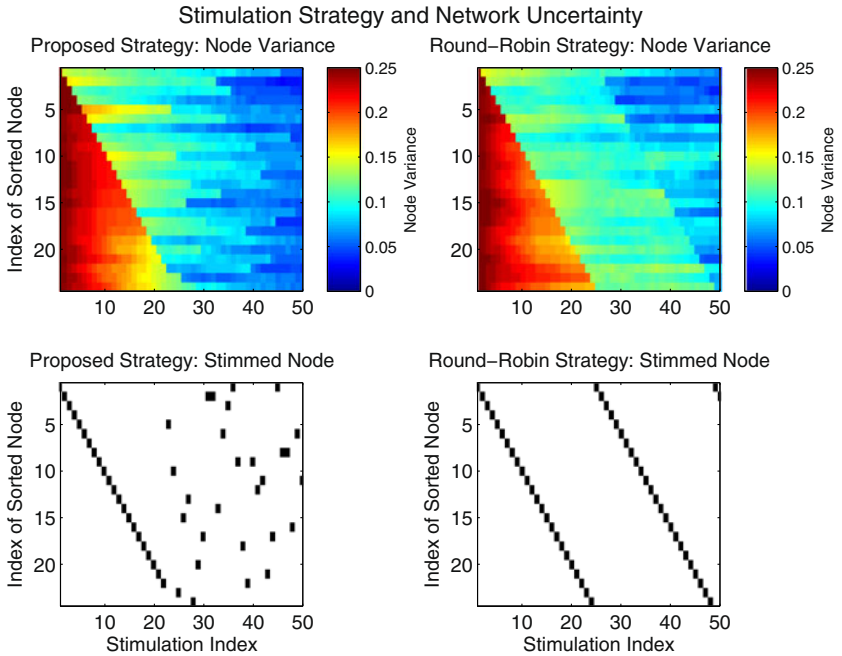

Fig. 6 *Top*: Node variance for the proposed methodology and the alternate approach as a function of stimulation index for the simulation of the clustered network using a detector with a probability of missed detection equal to 0.4. See Fig. 5, and the text for performance and simulation details. In each case, nodes are numbered according to the time of their first stimulation. The node variance is maximal when a node is stimulated for the proposed method and not always maximal when a node is stimulated in the alternate methodology. *Bottom*: Stimulation strategies. A *red pixel* indicates the stimulation index when a node is stimulated. The proposed strategy deviates from the round-robin strategy (*bottom plots*) and elicits an often pronounced change in the node variance (*top plots*) that is more pronounced with the proposed method than with the alternate method

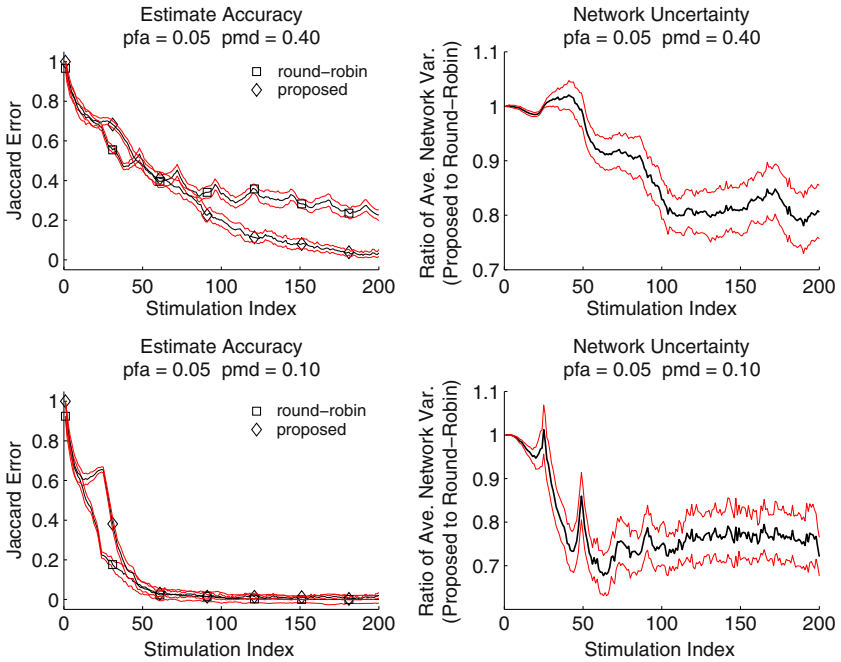

Fig. 7 *Left*: Accuracy of proposed vs more naïve network inference. For each of the 30 realizations, a 24 node network is simulated possessing a total of 276 possible edges. Of these possible connections only 14 exist. Most nodes are missing many connections with other nodes. The proposed method out-performs the more naïve network estimate by stimulation index 90 when the detector probability of missed detection is 0.4 (*upper row*) and is comparable to the more naïve network estimate when the detector probability is 0.1 (*lower row*). See Fig. 5 for a situation where the proposed method exhibits further advantage over the more naïve network estimator. *Right*: Network uncertainty comparison. Network variance, equal to the sum of the node variances, is lower when using the proposed method. See text for the definition of node and network variance

naïve method when the detector is poor (probability of missed detection = 0.4) and is equivalent after stimulation index 50 when the detector is good (probability of missed detection = 0.1). Network estimates computed with the proposed methodology are more certain than estimates computed with the more naïve approach, regardless of the probability of missed detection (right-half of Fig. 7). As the number of stimulations increases, estimate uncertainty of the proposed network estimator tends to approximately 70–80 % of the network variance of the estimates computed with the more naïve approach. In Fig. 8, the stimulation strategy employed with the relatively non-clustered network is shown. By comparing the change in node variance associated with stimulations of the non-clustered network presented in Fig. 8, with the change in node variance associated with stimulations of the more clustered network, Fig. 6, one sees that the change in node variance, and hence network estimate certainty, is much larger and pronounced in the situation where the clustered network is being estimated.

Simulation 3: The proposed methodology requires the specification of both the edge detector probability of false alarm and the edge detector probability of missed detection. While the probability of false alarm is controlled by the analyst, the probability of missed detection is typically unknown. In this final simulation, consisting of two-parts, the sensitivity of the proposed method to this assumption is explored by setting the probability of missed detection assumed by the network estimator to 0.1 in the first part (left-half Fig. 9) while the actual probability of missed detection is set to 0.1 and 0.4, respectively. In the second-part of the simulation, the probability of missed detection is set to 0.1 while the actual probability of missed detection is set to 0.1 and 0.4, respectively. In both parts of this simulation the realized networks possess network properties identical to those used to generate the clustered networks used in Simulation 1. The performance advantage, while reduced by the mis-specification, is still quite prominent when the proposed methodology operates in a scenario for which it is well-suited. As demonstrated in Fig. 9, performance degradation in less optimal scenarios is not substantial when due to mis-specification for the well-performing edge detector scenario (probability of missed detection equal to 0.1). Network estimates computed with the proposed methodology are more certain than estimates computed with the more naïve approach, regardless of

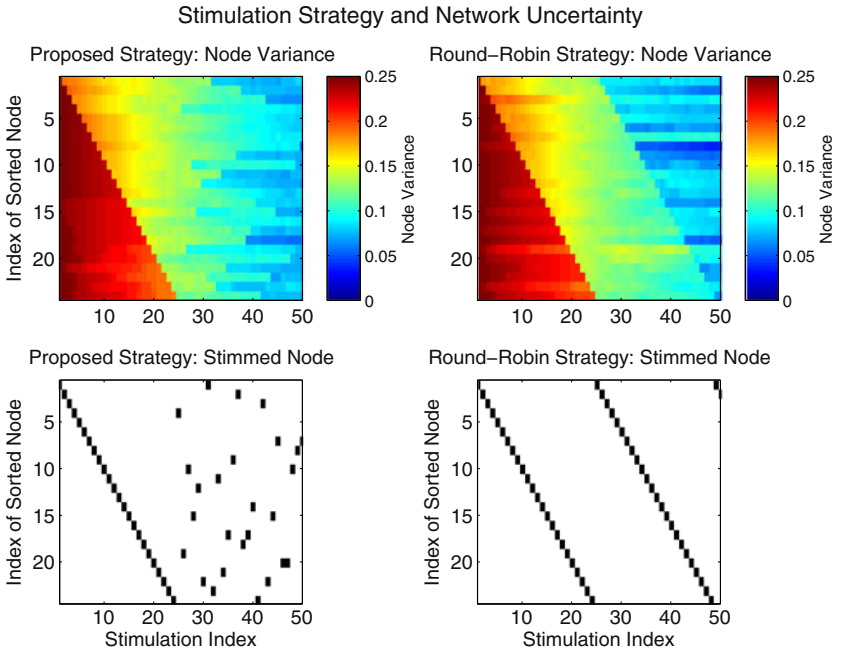

Fig. 8 *Top*: Node variance for the proposed methodology and the more naïve approach as a function of stimulation index for the simulation with the non-clustered network, and a detector probability of missed detection equal to 0.4. See Fig. 7, and the text for performance and simulation details. In each case, nodes are numbered according to the time of their first stimulation. The node variance is maximal when a node is stimulated for the proposed method and not always maximal when a node is stimulated in the alternate methodology. *Bottom*: Stimulation strategies. A *red pixel* indicates the stimulation index when a node is stimulated. The proposed strategy deviates from the round-robin strategy (*bottom plots*) and can elicit a pronounced change in the node variance (*top plots*) that is more pronounced with the proposed method than with the alternate method. Note that this effect is less in this situation than in the simulation of a more clustered network containing more edges, compare with Fig. 6

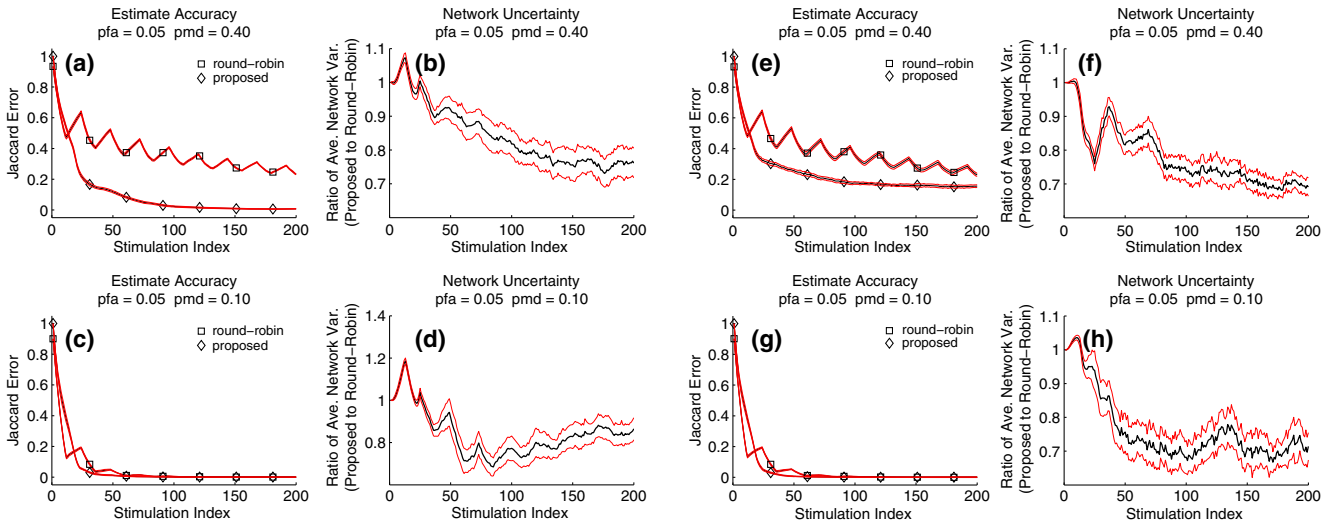

Fig. 9 Sensitivity to mis-specification of the edge detector probability of missed detection. Four plots on the *left half*: the probability of missed detection is thought, by the proposed network estimator, to be 0.4. Four plots on the *right half*: the probability of missed detection is thought, by the proposed network estimator, to be 0.1. Results corresponding to mis-specified detectors are plotted in plots (**c**), (**d**), (**e**), (**f**). Results corresponding to correctly specified edge detectors are displayed in plots (**a**), (**b**), (**g**), (**h**). These latter plots are included for comparison. Detector performance mis-specification results in reduced performance and changes in the estimated network variance. The performance advantage, while reduced, is still quite significant (compare plot (**a**) to plot (**e**)). These simulations are performed with the network specified in simulation 1. See the text and Fig. 5 for a description of the highly connected, clustered networks used in this simulation

probability of missed detection mis-specification (Parts (b), (d), (f), (h) of Fig. 9). As the number of stimulations increases estimate certainty of the proposed network estimator tends to approximately 70–80 % of the network variance of the estimates computed with the more naïve approach.

5 Discussion

5.1 Summary and potential applications

A method of inferring functional connectivity in a stimulate-and-record paradigm is proposed. This method is temporally-adaptive, disambiguates a source of non-identifiability when passively inferring functional network connectivity and reduces the number of required stimulations to achieve a given level of network uncertainty. The method is not specific to any particular stimulus or detector design. Indeed, while focus has been placed on potential ECoG implementation, the proposed paradigm is more general and is expected to be useful in a number of clinical applications. Examples of such paradigms include Deep Brain Stimulation (Perlmutter and Mink 2006; McIntyre and Hahn 2010) and simultaneous recording of EEG with application of Transcranial Magnetic Stimulation (Shafi et al. 2012). In each of these settings, the combination of stimulus, network, and nontrivial dynamics create a prime vehicle for the effective implementation of adaptive, stimulated network discovery.

In addition to clinical applications, the adaptive network scheme can be applied in basic experimental neuroscience. Emergent techniques such as optogenetics (Fenno et al. 2011) provide a means to stimulate specific populations of neurons and observe the resulting effects in other cells and spatial locations. The development of multi-electrode arrays for such stimulation and simultaneous measurement (Sparta et al. 2012) provides a direct platform for implementation of the proposed methodology to infer networks on a smaller, neuronal network scale.

5.2 Generalization

While the complete details of the following generalizations are the subject of future work, some central ideas are presented in the following.

5.2.1 Secondary activations

In the proposed methodology we have considered primary activations, i.e., the assumption that any detections are a function of direct connections emanating from the stimulated node. Any network may possess secondary activations. For example, consider stimulation applied to a single node ‘A.’ Node ‘A’ then affects node ‘B,’ which, in turn, affects node ‘C’. These activations can lead one to infer a connection between node ‘A’ and node ‘B’, and a connection between node ‘A’ and node ‘C’ when node ‘A’ is stimulated, even though a direct connection between node ‘A’ and node ‘C’ does not exist. In a sense, this inference is correct, since activity at node ‘A’ can influence activity at node ‘C’. However, in terms of representing physical connections, such secondary activations increase the number of false positives. In the above example, when the detector is run not just between the stimulated node, node ‘A’ and the other nodes, but also pairwise between all nodes on a given activation, one attains information about secondary activations. In particular, detector responses between node ‘B’ and node ‘C’ will be correlated with detector responses between node ‘A’ and node ‘C’ when node ‘A’ is stimulated. However, assuming there exists a change in the probability of missed detection with synaptic separation from the source of activation, these correlations will not be perfect. As the detector is applied to tertiary and quaternary connections, the correlation reduces as the probability of detection changes, perhaps due to a change in the strength of signal stimulation and efficacy of propagation. While not certain, principled incorporation of this information within the likelihood, Eq. (3), might lead to inference that is able to partially distinguish direct and indirect connections.

5.2.2 Multiple and simultaneous stimulation

In some settings, it may be desirable to stimulate multiple nodes simultaneously. If, after many stimulations, weakly connected subnetworks are discovered, stimulations can be applied simultaneously to each of the subnetworks, and these subnetworks inferred simultaneously and separately, with commensurate improvements in network inference. For more densely connected subnetworks, principled incorporation of multiple stimulations in the proposed inference paradigm is more complicated due to interaction effects, and is a topic for future research.

5.3 Extensions: network learning & control

This paper has focused on the problem of inferring connectivity through temporally-adaptive stimulation and observation. While useful in its own right, the methodology also provides a platform for exploring

solutions not only to infer the network, but to then use that information to guide *control*. Indeed, the chief objective of brain stimulation is to modulate or regulate certain types of aberrant activity. Incorporating a control objective into the methodology–for instance, reducing overall activity–may yield stimulation policies that simultaneously achieve real-time network adaptation and optimal control.

Acknowledgements K.Q.L. acknowledges support for this research from the Cognitive Rhythms Collaborative, NSF grant DMS-1042134 S.C. acknowledges support from NIH DP1-OD003646. S.C. holds a Career Award at the Scientific Interface from the Burroughs Wellcome Fund. M.A.K. holds a Career Award at the Scientific Interface from the Burroughs Wellcome Fund.

Appendix: Posterior update equation

$$\begin{aligned}
&\mathrm{P}\left(\mathbf{e}^{(k)}|\mathbf{d}^{(k)},\mathbf{s}^{(k)},\mathrm{H_k}\right)\\
&\quad\propto \mathrm{P}\left(\mathbf{d}^{(k)}|\mathbf{e}^{(k)},\mathbf{s}^{(k)},\mathrm{H_k}\right)\mathrm{P}\left(\mathbf{e}^{(k)}|\mathbf{s}^{(k)},\mathrm{H_k}\right)\ ,\\
&\quad=\mathrm{P}\left(\mathbf{d}^{(k)}|\mathbf{e}^{(k)},\mathbf{s}^{(k)}\right)\ \mathrm{P}\left(\mathbf{e}^{(k)}|\mathbf{s}^{(k)},\mathrm{H_k}\right)\ . \qquad (22)
\end{aligned}$$

The prior probability mass function of the edges, $\mathrm{P}\left(\mathbf{e}^{(k)}|\mathbf{s}^{(k)},\mathrm{H_k}\right)$ can be further decomposed by applying the Chapman–Kolmogorov equation.

$$\begin{aligned}
&\mathrm{P}\left(\mathbf{e}^{(k)}|\mathbf{s}^{(k)},\mathrm{H_k}\right)\\
&\quad=\sum_{\mathbf{c}\in C}\mathrm{P}\left(\mathbf{e}^{(k)}|\mathbf{e}^{(k-1)}=\mathbf{c},\mathbf{s}^{(k)},\mathrm{H_k}\right)\\
&\qquad\times\mathrm{P}\left(\mathbf{e}^{(k-1)}=\mathbf{c}|\mathbf{d}^{(k-1)},\mathbf{s}^{(k-1)},\mathrm{H_{k-1}}\right),\\
&\quad=\sum_{\mathbf{c}\in C}\mathrm{P}\left(\mathbf{e}^{(k)}|\mathbf{e}^{(k-1)}=\mathbf{c}\right)\\
&\qquad\times\mathrm{P}\left(\mathbf{e}^{(k-1)}=\mathbf{c}|\mathbf{d}^{(k-1)},\mathbf{s}^{(k-1)},\mathrm{H_{k-1}}\right), \qquad (23)
\end{aligned}$$

where C is the set of $2^{\mathrm{N_{edge}}}$ possible networks. Here it is assumed that $\mathbf{e}^{(k)}$ is conditionally independent of $\mathbf{s}^{(k)}$ and $\mathrm{H_k}$ given $\mathbf{e}^{(k-1)}$. Heuristically, this assumption implies that given knowledge of the network connections at stimulus index $k-1$, knowledge of the stimulus at the stimulation index k does not provide information about $\mathbf{e}^{(k)}$. This is a reasonable assumption since the stimulus at index k is determined from the posterior of $\mathbf{e}^{(k-1)}$.

Without a restriction upon C the sum in Eq. (23) is computationally intractable. As discussed in Section 3, this restriction is attained by assuming that the edges are independent of each other. With this assumption the probability mass functions factor and the prior probability mass function can be written,

$$\begin{aligned}
&\mathrm{P},\left(\mathbf{e}^{(k)}|\mathbf{s}^{(k)},\mathrm{H_k}\right)\\
&\quad=\prod_{j=1}^{\mathrm{N_{edge}}}\mathrm{P}\left((\mathbf{e}^{(k)})_j|(\mathbf{s}^{(k)})_j,\mathrm{H_k}\right)\\
&\quad=\sum_{\mathbf{c}\in C}\prod_{j=1}^{\mathrm{N_{edge}}}\mathrm{P}\left((\mathbf{e}^{(k)})_j|(\mathbf{e}^{(k-1)})_j=(\mathbf{c})_j\right)\\
&\qquad\times\mathrm{P}\left((\mathbf{e}^{(k-1)})_j=(\mathbf{c})_j|(\mathbf{d}^{(k-1)})_j,(\mathbf{s}^{(k-1)})_j,\mathrm{H_{k-1}}\right),\\
&\quad=\prod_{j=1}^{\mathrm{N_{edge}}}\sum_{c_j=0}^{1}\mathrm{P}\left((\mathbf{e}^{(k)})_j|(\mathbf{e}^{(k-1)})_j=c_j\right)\\
&\qquad\times\mathrm{P}\left((\mathbf{e}^{(k-1)})_j=c_j|(\mathbf{d}^{(k-1)})_j,(\mathbf{s}^{(k-1)})_j,\mathrm{H_{k-1}}\right). \qquad (24)
\end{aligned}$$

Combine Eq. (24) with Eq. (22), along with the edge independence assumption to obtain:

$$\begin{aligned}
&\prod_{j=1}^{\mathrm{N_{edge}}}\mathrm{P}\left((\mathbf{e}^{(k)})_j|\mathbf{d}^{(k)},\mathbf{s}^{(k)},\mathrm{H_k}\right)\\
&\quad\propto\prod_{j=1}^{\mathrm{N_{edge}}}\mathrm{P}\left((\mathbf{d}^{(k)})_j|\mathbf{e}^{(k)},\mathbf{s}^{(k)}\right)\times\sum_{c_j=0}^{1}\mathrm{P}\left((\mathbf{e}^{(k)})_j|(\mathbf{e}^{(k-1)})_j=c_j\right)\\
&\qquad\times\mathrm{P}\left((\mathbf{e}^{(k-1)})_j=c_j|(\mathbf{d}^{(k-1)})_j,(\mathbf{s}^{(k-1)})_j,\mathrm{H_{k-1}}\right). \qquad (25)
\end{aligned}$$

Thus, recursive update can be computed on an edge by edge basis,

$$\begin{aligned}
&\mathrm{P}\left((\mathbf{e}^{(k)})_j|\mathbf{d}^{(k)},\mathbf{s}^{(k)},\mathrm{H_k}\right)\\
&\quad\propto\mathrm{P}\left((\mathbf{d}^{(k)})_j|\mathbf{e}^{(k)},\mathbf{s}^{(k)}\right)\times\sum_{c_j=0}^{1}\mathrm{P}\left((\mathbf{e}^{(k)})_j|(\mathbf{e}^{(k-1)})_j=c_j\right)\\
&\qquad\times\mathrm{P}\left((\mathbf{e}^{(k-1)})_j=c_j|(\mathbf{d}^{(k-1)})_j,(\mathbf{s}^{(k-1)})_j,\mathrm{H_{k-1}}\right), \qquad (26)
\end{aligned}$$

for $j=1,\ldots,\mathrm{N_{edge}}$; greatly simplifying computations. This factoring allows for tractable computational inference, reducing both memory requirements and computation time.

References

Alarcon, G., Binnie, C.D., Elwes, R.D., Polkey, C.E. (1995). Power spectrum and intracranial eeg patterns at seizure onset in partial epilepsy. *Electroencephalography and Clinical Neurophysiology, 94*(5), 326–337.

Annegers, J.F. (2001). The epidemiology of epilepsy. In *The treatment of epilepsy: Principles and practice*. Lippincott Williams and Wilkins.

Conner, C.R., Ellmore, T.M., DiSano, M.A., Pieters, T.A., Potter, A.W., Tandon, N. (2011). Anatomic and electro-physiologic connectivity of the language system: a combined dti-ccep

study. *Computers in Biology and Medicine, 41*(12), 1100–1109 (Special Issue on Techniques for Measuring Brain Connectivity).

Dayan, P., & Abbott, L.F. (2005). *Theoretical neuroscience*. MIT Press.

Danzl, P., & Moehlis, J. (2008). Spike timing control of oscillatory neuron models using impulsive and quasi-impulsive charge-balanced inputs. In *Proceedings of the American control conference* (pp. 171–176).

de Curtis, M., & Gnatkovsky, V. (2009). Reevaluating the mechanisms of focal ictogenesis: the role of low-voltage fast activity. *Epilepsia, 50*(12), 2514–2525.

Destexhe, A., & Sejnowski, T.J. (2009). The wilson-cowan model, 36 years later. *Biological Cybernetics, 101*(1), 1–2.

Eden, U., Frank, L., Barbieri, R., Solo, V., Brown, E. (2004). Dynamic analysis of neural encoding by point process adaptive filtering. *Neural Computation, 16*(5), 971–998.

Enatsu, R., Piao, Z., O'Connor, T., Horning, K., Mosher, J., Burgess, R., Bingaman, W., Nair, D. (2012). Cortical excitability varies upon ictal onset patterns in neocortical epilepsy: a cortico-cortical evoked potential study. *Clinical Neurophysiology, 123*(2), 252–260.

Engel, J., Wiebe, S., French, J., Sperling, M., Williamson, P., Spencer, D., Gumnit, R., Zahn, C., Westbrook, E., Enos, B. (2003). Practice parameter: temporal lobe and localized neocortical resections for epilepsy: report of the quality standards subcommittee of the american academy of neurology, in association with the american epilepsy society and the american association of neurological surgeons. *Neurology, 60*(4), 538–547.

Fenno, L., Yizhar, O., Deisseroth, K. (2011). The development and application of optogenetics. *Annual Review of Neuroscience, 34*, 389–412.

Fisher, R.S., Webber, W.R., Lesser, R.P., Arroyo, S., Uematsu, S. (1992). High-frequency eeg activity at the start of seizures. *Journal of Clinical Neurophysiology, 9*(3), 441–448.

Friston, K. (1994). Functional and effective connectivity in neuroimaging: a synthesis. *Human Brain Mapping, 2*(1–2), 56–78.

Friston, K.J., Harrison, L., Penny, W. (2003). Dynamic causal modelling. *NeuroImage, 19*(4), 1273–1302.

Gibbs, F., Gibbs, E., Lennox, W. (2002). Epilepsy: a paroxysmal cerebral dysrhythmia. *Epilepsy & Behavior, 3*(4), 395–401.

Hasegawa, H. (2005). Synchronizations in small-world networks of spiking neurons: diffusive versus sigmoid couplings. *Physical Review E, Statistical, Nonlinear and Soft Matter Physics, 72*(5 Pt 2), 56139.

Juang, J.N. (1994). *Applied system identification.* PTR Prentice Hall, Inc.

Keller, C.J., Bickel, S., Entz, L., Ulbert, I., Milham, M.P., Kelly, C., Mehta, A.D. (2011). Intrinsic functional architecture predicts electrically evoked responses in the human brain. *Proceedings of the National Academy of Sciences of the United States of America, 108*(25), 10308–10313.

Keränen, T., Riekkinen, P.J., Sillanpää, M. (1989). Incidence and prevalence of epilepsy in adults in eastern Finland. *Epilepsia, 30*(4), 413–421.

Keränen, T., Sillanpää, M., Riekkinen, P.J. (1988). Distribution of seizure types in an epileptic population. *Epilepsia, 29*(1), 1–7.

Kramer, M.A., & Cash, S.S. (2012). Epilepsy as a disorder of cortical network organization. *The Neuroscientist, 8*(4), 360–372.

Kringelbach, M.L., Green, A.L., Owen, S.L.F., Schweder, P.M., Aziz, T.Z. (2010). Sing the mind electric—principles of deep brain stimulation. *European Journal of Neuroscience, 32*(7), 1070–1079.

Kringelbach, M.L., Jenkinson, N., Owen, S.L.F., Aziz, T.Z. (2007). Translational principles of deep brain stimulation. *Nature Reviews Neuroscience, 8*(8), 623–635.

Matsumoto, R., Nair, D.R., LaPresto, E., Bingaman, W., Shibasaki, H., Lders, H.O. (2007). Functional connectivity in human cortical motor system: a cortico-cortical evoked potential study. *Brain, 130*(1), 181–197.

Matsumoto, R., Nair, D.R., LaPresto, E., Najm, I., Bingaman, W., Shibasaki, H., Lders, H.O. (2004). Functional connectivity in the human language system: a cortico-cortical evoked potential study. *Brain, 127*(10), 2316–2330.

McIntyre, C., & Hahn, P. (2010). Network perspectives on the mechanisms of deep brain stimulation. *Neurobiology of Disease, 38*(3), 329–337.

Moro, E., & Lang, A.E. (2006). Criteria for deep-brain stimulation in Parkinson's disease: review and analysis. *Expert Review of Neurotherapeutics, 6*(11), 1695–1705.

Papoulis, A. (1984). *Probability, random variables and stochastic processes with errata sheet*. McGraw Hill Higher Education.

Perlmutter, J., & Mink, J. (2006). Deep brain stimulation. *Annual Review of Neuroscience, 29*, 229–257.

Rubinov, M., & Sporns, O. (2010). Complex network measures of brain connectivity: uses and interpretations. *NeuroImage, 52*(3), 1059–1069.

Schiff, N.D., Giacino, J.T., Kalmar, K., Victor, J.D., Baker, K., Gerber, M., Fritz, B., Eisenberg, B., Biondi, T., O'Connor, J., Kobylarz, E.J., Farris, S., Machado, A., McCagg, C., Plum, F., Fins, J.J., Rezai, A.R. (2007). Behavioural improvements with thalamic stimulation after severe traumatic brain injury. *Nature, 448*(7153), 600–603.

Schiff, S.J., Colella, D., Jacyna, G.M., Hughes, E., Creekmore, J.W., Marshall, A., Bozek-Kuzmicki, M., Benke, G., Gaillard, W.D., Conry, J., Weinstein, S.R. (2000). Brain chirps: spectrographic signatures of epileptic seizures. *Clinical Neurophysiology, 111*(6), 953–958.

Schiff, S.J., Sauer, T., Kumar, R., Weinstein, S.L. (2005). Neuronal spatiotemporal pattern discrimination: the dynamical evolution of seizures. *NeuroImage, 28*(4), 1043–1055.

Shafi, M.M., Westover, M.B., Fox, M.D., Pascual-Leone, A. (2012). Exploration and modulation of brain network interactions with noninvasive brain stimulation in combination with neuroimaging. *European Journal of Neuroscience, 35*(6), 805–825.

Sparta, D.R., Stamatakis, A.M., Phillips, J.L., Hovelsø, N., van Zessen, R., Stuber, G.D. (2012). Construction of implantable optical fibers for long-term optogenetic manipulation of neural circuits. *National Protocol, 7*(1), 12–23.

Sporns, O. (2010). *Networks of the Brain*. MIT Press.

Sunderam, S., Gluckman, B., Reato, D., Bikson, M. (2010). Toward rational design of electrical stimulation strategies for epilepsy control. *Epilepsy & Behavior, 17*(1), 6–22.

Valentín, A., Alarcón, G., Honavar, M., Seoane, J.J.G., Selway, R.P., Polkey, C.E., Binnie, C.D. (2005a). Single pulse electrical stimulation for identification of structural abnormalities and prediction of seizure outcome after epilepsy surgery: a prospective study. *Lancet Neurology, 4*(11), 718–726.

Valentín, A., Alarcón, G., García-Seoane, J.J., Lacruz, M.E., Nayak, S.D., Honavar, M., Selway, R.P., Binnie, C.D., Polkey, C.E. (2005b). Single-pulse electrical stimulation identifies epileptogenic frontal cortex in the human brain. *Neurology, 65*(3), 426–435.

Wang, Z., Kuruog andlu, E., Yang, X., Xu, Y., Huang, T. (2011). Time varying dynamic bayesian network for nonstationary events modeling and online inference. *IEEE Transactions on Signal Processing, 59*(4), 1553–1568.

Wilson, H.R., & Cowan, J.D. (1972). Excitatory and inhibitory interactions in localized populations of model neurons. *Biophysical Journal, 12*, 1–24.

Wilson, H.R., & Cowan, J.D. (1973). A mathematical theory of the functional dynamics of cortical and thalamic nervous tissue. *Kybernetik, 13*, 55–80.

Zarrelli, M.M., Beghi, E., Rocca, W.A., Hauser, W.A. (1999). Incidence of epileptic syndromes in Rochester, Minnesota: 1980–1984. *Epilepsia, 40*(12), 1708–1714.

Zhang, H., Benz, H., Bezerianos, A., Acharya, S., Crone, N., Maybhate, A., Zheng, X., Thakor, N. (2010). Connectivity mapping of the human ecog during a motor task with a time-varying dynamic bayesian network. In *2010 annual international conference of the IEEE in engineering in medicine and biology society (EMBC)* (pp. 130–133).